Metallogr. Microstruct. Anal. (2013) 2:140–147
DOI 10.1007/s13632-013-0072-x

TECHNICAL ARTICLE

New Metallographic Method for Estimation of Ordering and Lattice Parameter in Ternary Eutectic Systems

A. Dennstedt · L. Ratke · A. Choudhury · B. Nestler

Received: 5 February 2013 / Revised: 27 March 2013 / Accepted: 26 April 2013 / Published online: 10 May 2013

Abstract Ternary eutectics develop a rich variety of microstructures depending on the solidification conditions. This article describes a new procedure to analyze the three-phase arrangement in metallographic sections following solidification; this method provides a clear definition of both the interphase spacing and the degree of ordering. Distance and angle between the phase areas are calculated after determination of the centers of mass for each phase area. A polar plot of these data allows an easy determination of the spacing and the order. The new method is discussed with both experimental as well as simulated microstructure images. It is first tested on artificial phase arrangements, which are fully ordered, semi-ordered, or random.

Keywords Structural characterization · Alloys · Microstructure · Microscopy · Al–Ag–Cu

Introduction

In three component systems with a ternary eutectic point, three phases can solidify simultaneously from the melt in a eutectic reaction. In simple binary eutectic systems only two morphologies are possible, either lamellae or fibrous. However, ternary eutectic alloys exhibit a much richer variety of possible morphologies. For instance, the three phases can be arranged in fibers, two fibers embedded in a lamella, two lamellae embedded in a matrix, a ladder structure of two phases in a matrix, two phases parallel and one phase orthogonal to it and many others. The phases can be arranged almost regularly until completely disordered and these might have simple surface geometries like circular, ellipsoid, rectangular in a cross section, or very complex folded ones [1–3]. Thus, these systems are ideally suited for studying the fundamental science of a highly complex, multiphase solidification process.

Al–Ag–Cu is often used as model system for these kinds of studies. The phase diagram has recently been validated very carefully [4] and the three phases solidifying, namely the Ag_2Al-, the Al_2Cu θ-phase, and the α-aluminum solid solution phase, grow in a non-facetted manner (in contrast to, for instance, the eutectic in the AlSiCu system). As the thermodynamics in this system are also well known, 3D phase-field modeling can be utilized to probe stability limits and complex pattern formation, and to compare the simulated microstructures with real microstructures.

The microstructures observed in AlAgCu eutectic alloys depend on solidification velocity and composition, as to be expected from the theory of eutectics [3, 5, 6]. McCartney et al. [7] identified a "semi-regular brick-type structure" for the Al–Ag–Cu system. In contrast to this, several different structures, even in one cross section, have been identified by the authors in previous studies on this alloy system [3, 8]. The structures were classified as ordered and irregular, but also spirals, cobble pavement structures, and others were found.

One essential issue in ternary eutectics is how to unambiguously describe the structure and transition between the observed varieties, such that one can try to understand the physical mechanisms behind them utilizing microstructure modeling. Appropriate descriptors of

A. Dennstedt (✉) · L. Ratke
Institut für Materialphysik im Weltraum, Deutsches Zentrum für Luft- und Raumfahrt (DLR), 51170 Cologne, Germany
e-mail: anne.dennstedt@dlr.de

A. Choudhury · B. Nestler
Institut für Angewandte Materialien, Karlsruhe Institut für Technologie, 76131 Karlsruhe, Germany

microstructures include the distances between the phases, distance between like and unlike phases, the shape factor of the phase in a cross section, the orderly arrangement of phases, area fraction, grain orientation, density of triple points, and angle distribution at triple points. In attempting to describe the ternary microstructure, a description of the separation and distances between two areas of the same phase in simulated as well as in real cross sections is developed. In collaboration with this description, an analysis of the orderly arrangement is possible. The measure should include distances in different directions, largely in horizontal and in vertical direction. In this article, a new method will be presented which allows for a rapid determination of an average distance in different directions between (nearly) regular ordered particles.

Experimental

Ag–Al–Cu alloys of near-eutectic composition were cast into stainless steel molds. Subsequently, rods were machined to fit the ARTEMIS facility. The ARTEMIS facility was used for directional solidification and is described in detail in [9]. Samples presented in this publication were solidified with velocities of 0.08, 0.11, or 0.2 μm/s and an applied gradient of 2.2 K/mm. Cross sections of the directionally solidified rods were prepared using standard metallographic procedures. Scanning electron microscope (SEM) images using the backscattered mode (Fig. 1a–c) show microstructures of a ternary eutectic perpendicular to the solidification direction. The contrast between the three phases is excellent: the white phase is the Ag_2Al phase, the black one the solid solution α-Al, and the medium gray phase is the Al_2Cu phase. The figures show that the Ag- and the Cu-rich phase are partially arranged in a series like a ladder or bricks and the α-Al phase is always in between.

Experimentally, several types of phase arrangements are observed. Different processing conditions (especially velocity, velocity jumps and the thermal gradient), as well as slight variations of alloy composition, will result in variations in the microstructure pattern. There always is a sedimentation or segregation of the heavier Ag and Cu atoms in the melt above the solidification front, leading already to axial variations in composition, and thus phase fractions and likely also leading to variations in microstructure. To explore the possible microstructures, and thereby develop an understanding of the underlying mechanisms/correlations between the observed patterns and the imposed growth conditions, a state-of-the art phase-field method was utilized. 3D phase-field simulations were performed for a symmetric phase diagram as well as a slightly asymmetric phase diagram, where the

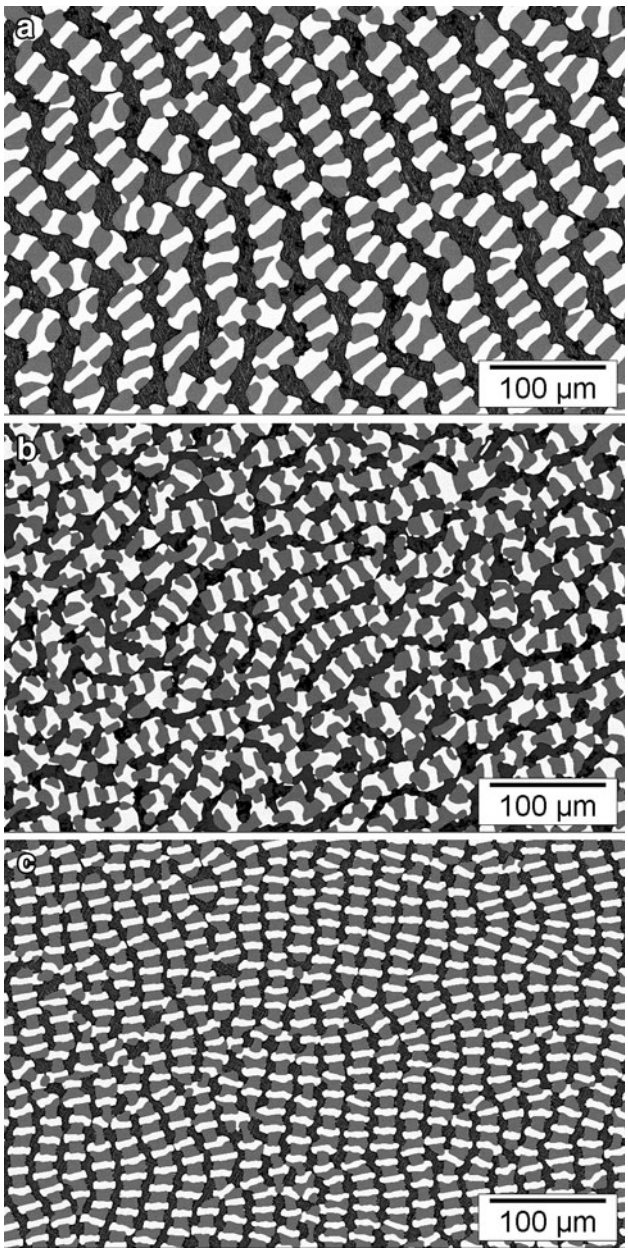

Fig. 1 SEM images of Al–Ag–Cu alloys containing Ag_2Al (*white*), Al_2Cu (*gray*), and Al (*black*) phase (compare phase diagram in [4]). Alloy solidified with (**a**) 0.08 μm/s and 2.2 K/mm, (**b**) 0.11 μm/s and 2.2 K/mm, and (**c**) 0.2 μm/s and 2.2 K/mm

asymmetry is introduced by increasing the volume fractions in favor of one of the solid phases, while keeping the volume fractions of the remaining two solid phases equal. Starting from a random initial setting, with the alloy composition fixed at the eutectic, two different microstructures were obtained for the symmetric and the asymmetric phase diagrams. For a purely symmetric phase diagram the simulations resulted in a hexagonal pattern which seems to be the most stable arrangement (Fig. 2a), while for the slightly asymmetric phase diagram, a regular

brick like structure shown in Fig. 2(b) was obtained. A difference in volume fraction of each phase can also be induced through a change in the alloy composition. The pattern, shown in Fig. 2(c), was obtained for an off-eutectic composition in the symmetric phase diagram. The above simulations structures have been published in a preceding article [10].

Results and Discussion

Images of real ternary eutectics, as well as simulated ones, were used for evaluation of the new method shown in this article. The SEM images in Fig. 1(a–c) show structures obtained via directional solidification of Al–Ag–Cu melt of near-eutectic composition. In Fig. 1(a), the phase particles are regularly arranged and such a pattern can be called a ladder structure [3, 6, 7]. The structure consists of two lamellas. One lamella is made of Al, the other one is composed of the two intermetallic phases in a lamellar arrangement. Such an arrangement was discussed by Himemiya and Umeda [6]. They defined a parameter ε, which is the ratio of λ_2/λ_1. Here, λ_1 is the distance between the lamellas of the α-Al solid solution and λ_2 the distance between Ag_2Al and Al_2Cu in the intermetallic lamellae. To simplify the discussion here, in this article, the distance between the intermetallic lamellas was used as λ_1. Thus, it is possible to use one of the intermetallic phases for the estimation of both distances λ_1 and λ_2 (compare arrows in Fig. 2b). Himemiya and Umeda [6] calculated a theoretical value of 0.45. However, with images of McCarntey they obtained a value of 0.75. Genau and Ratke [3] found experimentally a value of 0.62. Figure 2(a–c) shows simulated structures which again include three different phases represented as white, gray, and black areas. Pattern of the phase particles were generated. These images, in addition to the images of the real microstructures, are used to test the new method presented in this study.

Three different types of phase particles occur in the images. To explain the new method, the silver-rich particles shown as white areas in the images are considered. The software analySIS pro [11] was used to determine the center of mass of every Ag_2Al particle. These points define the position of the particles and create a more or less

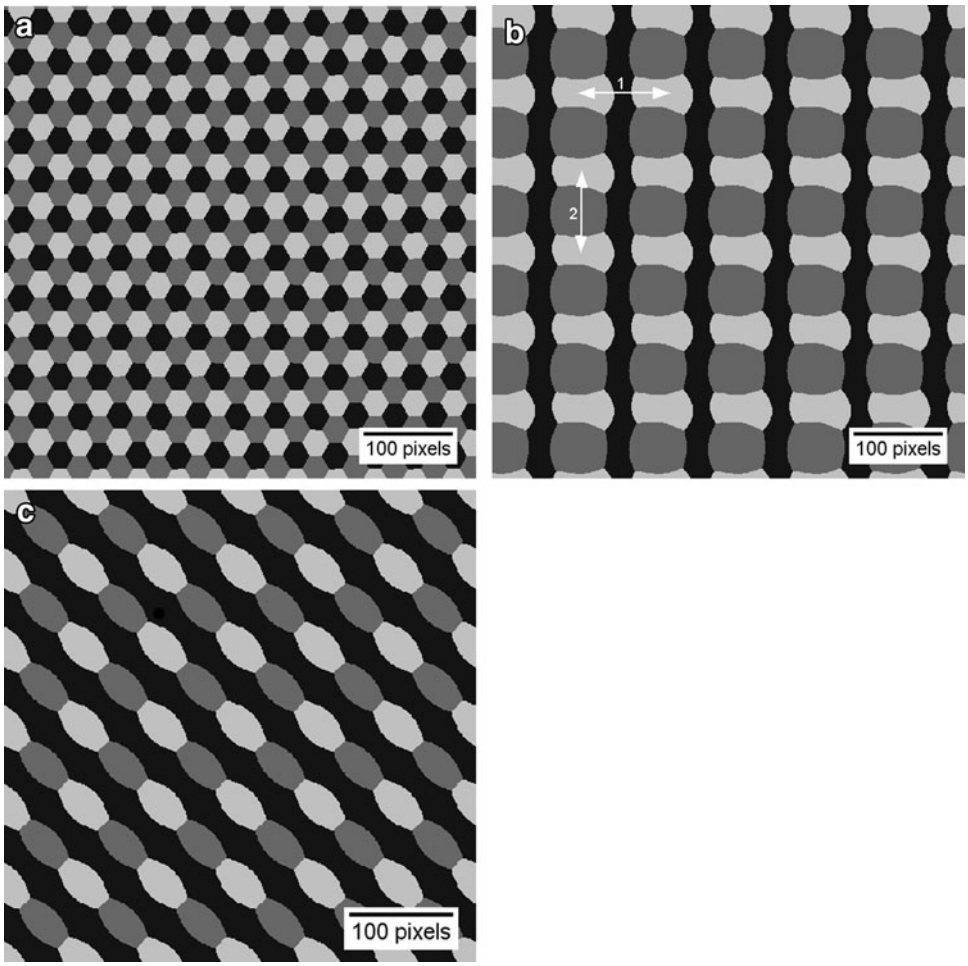

Fig. 2 Structures obtained during 3D simulation of directional solidification [10]. (**a**) A hexagonal pattern is formed upon solidification from a random initial setting for a symmetric phase diagram at the ternary eutectic composition. (**b**) A semi-regular brick like structure is obtained upon solidification from a random setting for an asymmetric phase diagram at the eutectic composition. The *arrows* show the use of λ_1 (1) and λ_2 (2) in this article. (**c**) An alternating series of αβ lamellae interspersed between the matrix is obtained starting from an off-eutectic composition. All figures are tiled six times to clarify the underlying pattern

regular lattice. Figure 3 shows a lattice of points with labels for both distances x and y as well as the angle γ between the two directions. In addition, two points P1 and P2 are labeled together with their distance d and the definition of the angle ϕ between them. The distance between these two points is calculated according to Eq. (1).

$$d = \sqrt{(\Delta x)^2 + (\Delta y)^2} \tag{1}$$

The angle ϕ is calculated with the function

$$\varphi = \arctan \frac{\Delta y}{\Delta x}. \tag{2}$$

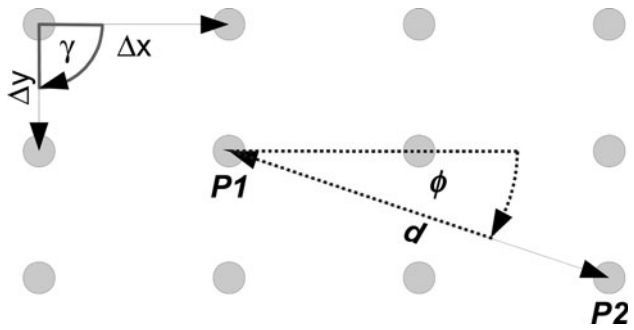

Fig. 3 Scheme of a lattice and its parameters used for the calculations. Δx and Δy are the distances between two points in x- and y-directions, γ is the angle between these two lattice directions, ϕ and d are the angle and the distance between the two considered points labeled as P1 and P2

First, three different hypothetical cases of point arrangements are considered (Fig. 4a–c). The first case is a lattice with regular distances between the points in both directions (Fig. 4a). In the second case, shown in Fig. 4(b), the distances between the points in the x-direction vary, whereas the distances in the y-direction remain constant. For the third case, neither the x nor the y-direction show regular distances (Fig. 4c). All distances and all angles were calculated for every single point with a code written in Octave [12]. Calculated values for the three cases discussed were plotted in a polar coordinate system shown in Fig. 5(a–c). The calculated distance was used as the radius and the calculated angle was used as the azimuth. In the first case (Fig. 5a) of the regular lattice, a pattern of points appeared in this polar plot. One can directly read the distance between the points in both the directions. In each of the two directions, the distance from the pole of the plot to the first point is the single distance between the points of the lattice in the direction considered. The distance between the pole and the second point reflects the doubled distance between points in the direction considered, and so on.

In the second case (Fig. 5b) of the semi-regular lattice, the distance can only be read in one direction. The third case showed a completely irregular arrangement of points. The pattern observed in this polar coordinate system has the appearance of a cloud and an exclusive distance cannot be detected. In this respect, the polar plots of distances and

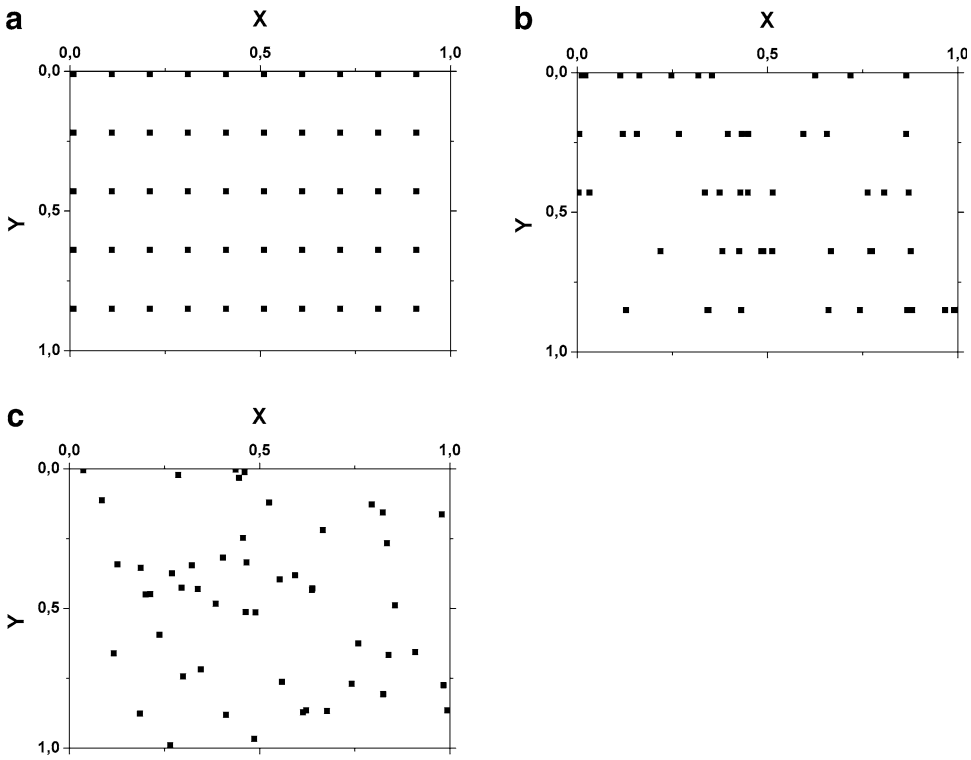

Fig. 4 Theoretical lattices used for first calculations and plots. Lattice has regular distances between the points (**a**) in both directions, (**b**) in y-direction, and (**c**) in none of the directions

angles clearly showed the transition from a regular, ordered structure to an irregular unordered one.

The polar plots shown in Fig. 5(d–f) were obtained for the Ag_2Al particles in the images of the real microstructures shown in Fig. 1(a–c). The resulting patterns in the pole plots shown in Fig. 5(d, f) show some detectable pattern of points. Thus, the determination of average distances in both directions is possible; these values are listed in Table 1 together with the calculated parameter ε. The arrangement of the Ag_2Al particles is too irregular in the case of Fig. 1(b) to obtain a usable pattern in the resulting pole plot (Fig. 5e). There is a region with some ladder structure in the center of the image shown in Fig. 1(b). However, large regions show an irregular arrangement of the Ag_2Al phase particles. In these regions, each Ag_2Al particle has a different surrounding in comparison to other Ag_2Al particles. The only point which can be extracted from the plot in Fig. 5(e) is a minimal distance between particles, which can be read from the points with the lowest values of the radius.

In addition to the distance between the particles, plots in Fig. 5(d, f) show the direction or orientation of the lamellas. The direction is reflected by the dominant linear accumulation of points. Thus, an orientation of about 60° is observed in the polar plot in Fig. 5(d) generated by the image in Fig. 1(a). In contrast, for Fig. 1(c), an orientation of 90° is indicated in Fig. 5(f). The curvature of the less dominant linear accumulation of points in Fig. 5(f) is

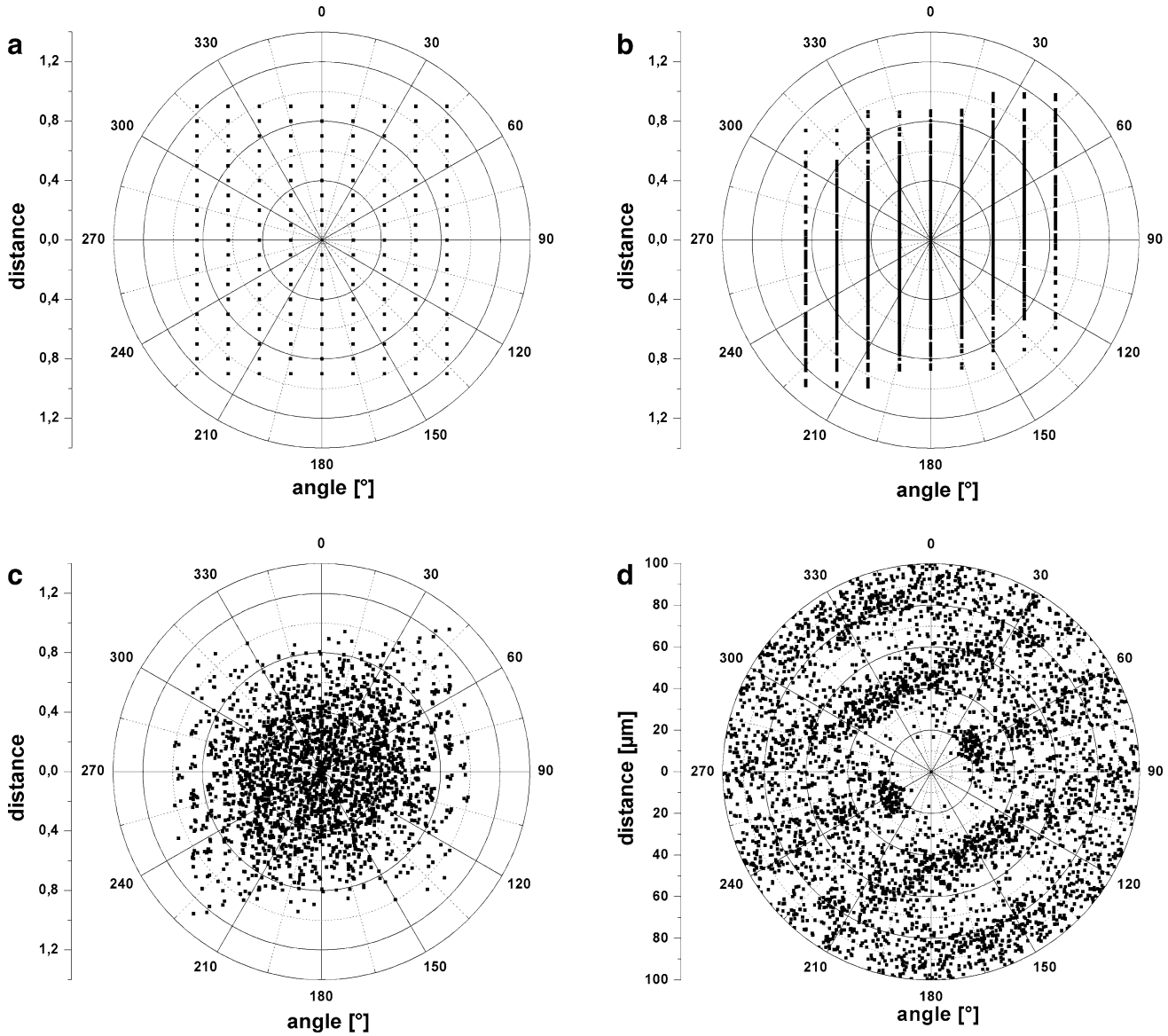

Fig. 5 Patterns in polar coordinate system obtained after calculation of distances and angles. (**a–c**) obtained with the lattices shown in Fig. 4(**a–c**), (**d–f**) obtained with the experimental images shown in Fig. 1(**a–c**), and (**g–i**) obtained with the simulated images shown in Fig. 2(**a–c**)

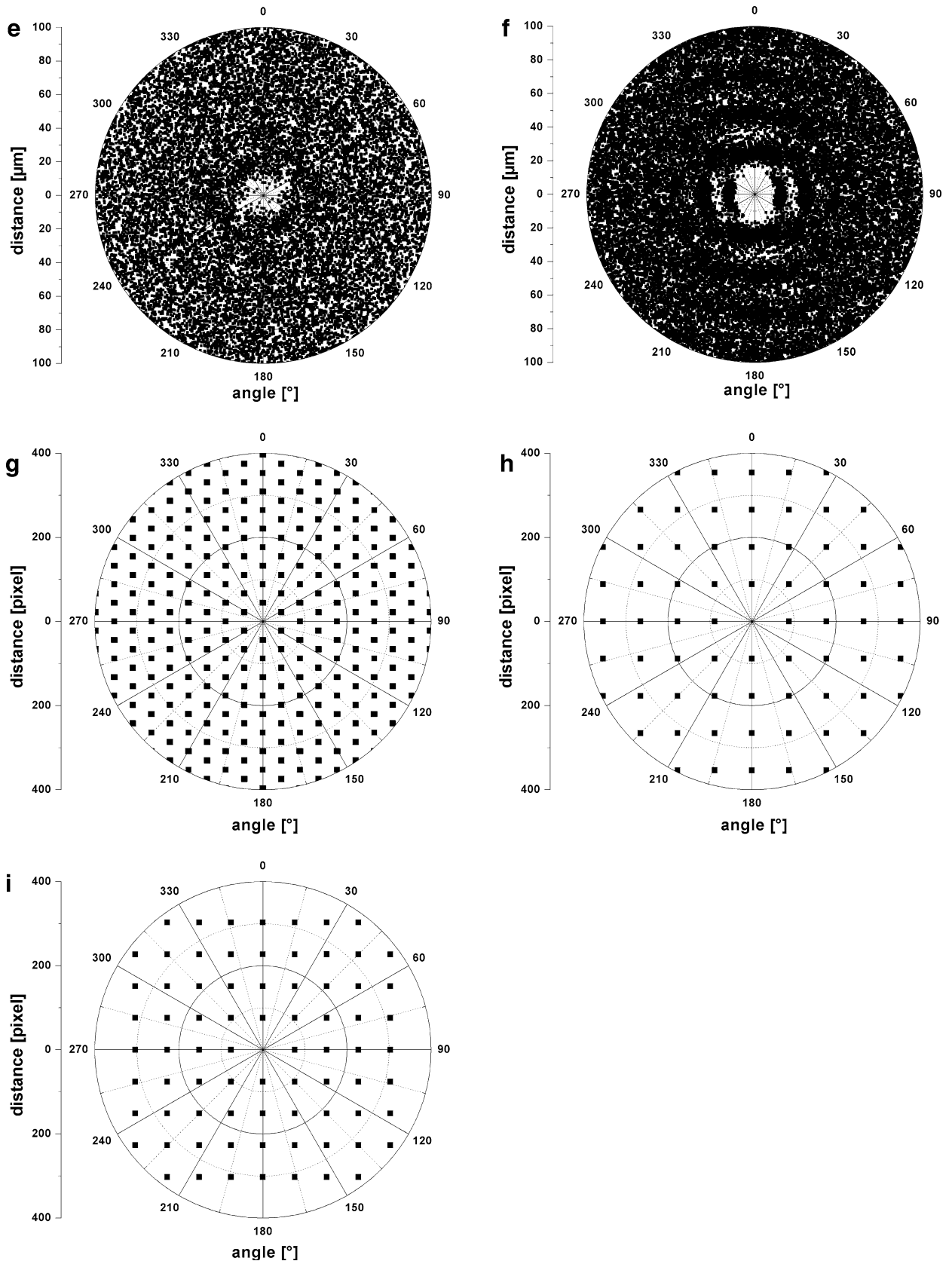

Fig. 5 continued

caused by the mixed misalignment between the Ag_2Al particles in the different intermetallic lamellas. If there were only one type of misalignment between the lamellas, then the centers of mass would form a lattice of points comparable to that one shown in Fig. 3, but with an angle γ differing from 90°. In that more simple case, the less dominant linear accumulation would not be curved and the angle γ could be read from the difference between the angles of both accumulation lines.

Figure 5(g–i) shows polar plots obtained by evaluation of the white phase particles in the simulated structures in Fig. 2(a–c). All patterns show a high degree of order. In the case of Fig. 2(a), every white particle has six nearest white particles. This is reflected in the polar plot with six points surrounding the pole. A detailed view to the *n*-fold distances in the directions connected to these points reveals a deviation from 60°. This deviation is caused by a small elongation of the particles. In Fig. 5(h, i), the patterns obtained are very similar. In both cases, the centers of mass are arranged in a squared fashion. The polar plots differ only in the distances between the single points. A discrimination between these two simulated structures is possible if one considers distances and angles between the two different phases shown as white and gray areas in Fig. 2(b, c). For each white area in Fig. 2(b, c), the distances to all gray areas were calculated and plotted in Fig. 6(a, b). The patterns obtained are similar to that in Fig. 5(h, i). However, a centered point appeared and the origin is shifted in different ways. In the case of Fig. 2(b), the obtained pattern shown in Fig. 6(a) is shifted only in one direction, whereas the structure shown in Fig. 2(c) resulted in a pattern which is shifted in two directions perpendicular to each other (Fig. 6b).

In general, the development of patterns in the polar coordinate system can be explained by the positioning of every single point to the pole of the system and then plotting all points being neighbors to this point. If the surroundings of the points are equal, a smooth pattern arises. The more different the surroundings are, the more chaotic the resulting pattern will be. Thus, this evaluation method provides a quick method to distinguish between ordered and disordered structures. The determination of average distances, directions as well as angles between directions is possible by evaluation of patterns of ordered structures.

Table 1 Distances and parameter ε estimated in the polar plots shown in Fig. 5(d, f)

SEM image	λ_1 (μm)	λ_2 (μm)	ε
Figure 1(a)	24.5 ± 0.2	15.7 ± 0.2	0.64 ± 0.01
Figure 1(c)	42.7 ± 0.4	24.5 ± 0.2	0.58 ± 0.01

Conclusions

In this article, a method is shown to estimate distances in a more or less ordered arrangement of areas in a 2D image. The surroundings of every phase particle are plotted around the pole of a polar coordinate system. Due to the overlap of these points, an accumulation of lines appears in the polar plots. These lines reflect both distances between the particles as well as the orientation of the rows of the particles. Decreasing the order in the microstructure image from

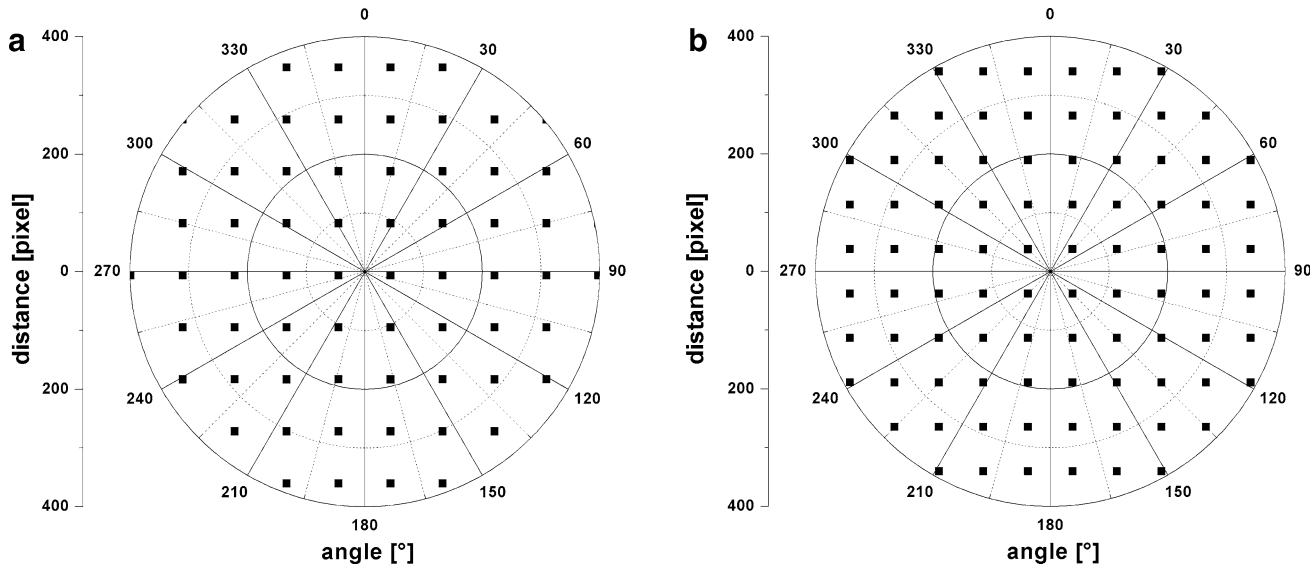

Fig. 6 Patterns obtained by calculation of distances and angles between areas of different phases. (**a**) obtained with the simulated image shown in Fig. 2(**b**), and (**b**) obtained with the simulated image shown in Fig. 2(**c**)

regular, to semi-regular, to irregular arrangements, results in a concomitant transition in the polar plot from a regular pattern to a disordered cloud of points.

This procedure allows for a simple and direct evaluation of both the average distances in a microstructure and the order in the arrangements of phase areas. It can be used for a variety of microstructures where any type of phase particles or areas are arranged, such as a dendritic structure in 2D cross sections to reveal differences between ordered and disordered arrangements and to easily estimate the primary stem separation [13].

Acknowledgments The authors gratefully acknowledge the financial support by the Deutsche Forschungsgemeinschaft under Contract Numbers RA537/14-1 and NE822/14-1.

References

1. U. Hecht, L. Gránásy, T. Pusztai, B. Böttger, M. Apel, V. Witusiewicz, L. Ratke, J. De Wilde, L. Froyen, D. Camel, B. Drevet, G. Faivre, S.G. Fries, B. Legendre, S. Rex, Multiphase solidification in multicomponent alloys. Mater. Sci. Eng. R **46**(1–2), 1–49 (2004)
2. D. Lewis, S. Allen, M. Notis, A. Scotch, Determination of the eutectic structure in the Ag–Cu–Sn system. J. Electron. Mater. **31**(2), 161–167 (2002)
3. A. Genau, L. Ratke, Morphological characterization of the Al–Ag–Cu ternary eutectic. Int. J. Mater. Res. **103**(4), 469–475 (2012)
4. V. Witusiewicz, U. Hecht, S. Fries, S. Rex, The Ag–Al–Cu system II. A thermodynamic evaluation of the ternary system. J. Alloys Compd. **387**(1–2), 217–227 (2005)
5. K. Jackson, J. Hunt, Lamellar and rod eutectic growth. Trans. Metall. Soc. AIME **236**, 1129–1142 (1966)
6. T. Himemiya, T. Umeda, Three-phase planar eutectic growth models for a ternary eutectic system. Mater. Trans. JIM **40**(7), 665–674 (1999)
7. D.G. McCartney, R.M. Jordan, J.D. Hunt, The structures expected in a simple ternary eutectic system: part II. The Al–Ag–Cu ternary system. Metall. Trans. A **11**(8), 1251–1257 (1980)
8. A. Dennstedt, L. Ratke, Microstructures of directionally solidified Al–Ag–Cu ternary eutectics. Trans. Indian Inst. Met. **65**(6), 777–782 (2012)
9. J. Alkemper, S. Sous, S. Stöcker, L. Ratke, Directional solidification in an aerogel furnace with high resolution optical temperature measurements. J. Cryst. Growth **191**(1–2), 252–260 (1998)
10. A. Choudhury, M. Plapp, B. Nestler, Theoretical and numerical study of lamellar eutectic three-phase growth in ternary alloys. Phys. Rev. E (2011). doi:10.1103/PhysRevE.83.051608
11. analySIS pro, Olympus Soft Imaging Solutions GmbH (1986–2007). http://www.olympus-sis.com. Accessed 5 Feb 2013
12. http://www.gnu.org/software/octave/. Accessed 5 Feb 2013
13. S. Ahrweiler, L. Ratke, J. Lacaze, Microsegregation and microstructural features of directionally solidified AlSi and AlSiMg alloys. Adv. Eng. Mater. **5**, 17–23 (2003)